Three-Dimensional Numerical Simulation of Segregation in Dense Suspensions

Ilinca, Florin; Hetu, Jean-Francois

Three-Dimensional Numerical Simulation of Segregation in Dense Suspensions

Florin Ilinca and Jean-François Hétu

National Research Council, Industrial Materials Institute
75 de Mortagne, Boucherville, Québec, Canada, J4B 6Y4

Abstract. The ability to predict segregation of the solid phase in processes such as powder injection molding and injection molding of semi-solid materials is of special interest since such phenomenon affects the final properties and characteristics of the molded parts. In powder injection molding, for example, defects appear very often in the debinding and sintering stages but are caused by filling problems and determined by a non-uniform distribution of the solid particles within the molded part. In this paper we propose a 3D numerical solution algorithm for the simulation of particle migration in dense suspensions. The particle migration is modeled using the diffusion flux model and integrated into the NRC's 3D injection molding software. The solution algorithm is validated by solving flow problems for which experimental and numerical data are available: circular Couette flow, piston driven flow and sudden contraction-expansion flow. Since it is observed that the piston movement in the sleeve can induce particle migration even before the material enters the cavity, an ALE formulation is also developed to include the piston movement in molding simulations. The ALE formulation is first compared with an Eulerian solution for the case of the piston driven flow problem. Then the approach is applied to injection molding problems and the segregation inside the molded parts is studied.

Keywords: Dense suspensions, 3D Modeling, Finite Elements, Segregation, Diffusive flux model.
PACS:

INTRODUCTION

The ability to predict segregation of the solid phase in processes such as powder injection molding (PIM) is of special interest since such phenomenon affects the final properties and characteristics of the molded parts. PIM defects appear very often in the debinding and sintering stages but are often caused by filling problems and determined by a non-uniform distribution of the solid particles within the solution. Inhomogeneous particle distribution affects the apparent viscosity and thus the flow during filling. This distribution may also affect the part deformation during sintering and consequently the final part geometry.

Various models have been proposed to describe the separation of the solid and fluid constituents in dense suspensions. In mixture models each constituent is considered as distinct specie of a mixture. The development of the mixture formulation is done by writing the conservation equations for each phase involved in the system. Two sets of momentum, mass and energy conservation equations are therefore written, one set for the liquid phase and one for the solid phase. These coupled equations can be solved directly [1,2]; however, for computational efficiency reasons, it is usually further simplified using phase mixture rules. By doing so, the two sets of conservation equations are reduced to one set of conservation equations into which the unknowns are the average mixture velocity, pressure and temperature; the local concentration of the mixture is computed using an additional phase concentration equation [3,4].

PIM can also be modelled using dense suspension models. Dense suspension models have been developed to predict shear induced particle segregation. Conceptually, such models assume that particle-particle collision occurring in the suspension is the main driving force for phase separation. High-shear regions have a higher collision probability than low shear regions, thus based on probabilistic arguments, particles tends to migrate from the high shear flow regions to the low shear flow regions. Phillips *et al.* [5] introduced the diffusive flux model based on the concept of particle concentration diffusion. Experimental validation of the model for simple one- or two-dimensional problems is shown in

Refs. [6,7]. The suspension balance model was first introduced by Nott and Brady [8] who introduced the concept of suspension 'temperature'. Morris and Boulay [9] modified the model to take into account the effect of the normal stress difference, whereas Fang et al. [10] used a flow aligned tensor to model the normal stress difference for both diffusive flux model and suspension balance model. Experimental validation of both diffusive flux and suspension balance models is shown in Refs. [11,12].

In this paper we propose a 3D numerical solution algorithm for the simulation of particle migration in dense suspensions. The particle migration is modeled using the diffusion flux model proposed by Phillips et al. [5]. The particle migration model is integrated into the NRC's 3D injection molding software [13]. The solution algorithm is validated by solving flow problems for which experimental and numerical data are available: circular Couette flow, piston driven flow and sudden contraction-expansion flow [6,10]. An ALE formulation is also developed to treat the piston movement in injection molding problems. The ALE formulation is first compared with an Eulerian solution for the case of the piston driven flow problem. Then the approach is applied to injection molding problems and the segregation inside the molded parts is studied.

MODEL EQUATIONS

The flow of incompressible fluids is described by the Navier-Stokes equations

$$\rho\left(\frac{\partial \mathbf{u}}{\partial t}+\mathbf{u}\cdot\nabla\mathbf{u}\right)=-\nabla p+\nabla\cdot(2\eta D_{ij}), \qquad (1)$$

$$-\nabla\cdot\mathbf{u}=0, \qquad (2)$$

where η is the apparent viscosity of the suspension and $D_{ij}=(\nabla\mathbf{u}+(\nabla\mathbf{u})^T)/2$ is the strain rate tensor.

Heat transfer is modeled by the energy equation:

$$\rho c_p\left(\frac{\partial T}{\partial t}+\mathbf{u}\cdot\nabla T\right)=\nabla\cdot(k\nabla T)+2\eta D_{ij}D_{ij}. \qquad (3)$$

In the above equations, t, $\mathbf{u}$, p, T, ρ, η, c_p and k denote time, velocity, pressure, temperature, density, viscosity, specific heat and thermal conductivity respectively.

For instance the viscosity is considered as a function of the solid fraction as given by

$$\eta=\eta_r\eta_s,\ \ \eta_r=\left(1-\bar{\phi}\right)^{-1.82}, \qquad (4)$$

where η_s is the viscosity of the suspension (liquid phase), η_r is the relative viscosity of the mixture with respect to that of the suspension, and $\bar{\phi}$ denotes the normalized solid fraction, $\bar{\phi}=\phi/\phi_m$. Here ϕ denotes the solid fraction and ϕ_m its maximum value (ϕ_m=0.68 for the present work).

The segregation of solid particles is modeled by the diffusive flux model of Phillips et al. [5]. The solid fraction is therefore obtained by solving the transient advective-diffusive equation

$$\frac{\partial\phi}{\partial t}+\mathbf{u}\cdot\nabla\phi=-\nabla\cdot\mathbf{N} \qquad (5)$$

where the diffusive flux $\mathbf{N}$ is given by

$$\mathbf{N}=\mathbf{N}_c+\mathbf{N}_\eta, \qquad (6)$$

$$\mathbf{N}_c=-a^2\phi K_c\nabla(\dot{\gamma}\phi), \qquad (7)$$

$$\mathbf{N}_\eta=-a^2\phi^2\dot{\gamma}K_\eta\nabla(\ln\eta). \qquad (8)$$

In the above equations a represents the radius of solid particles in the suspension, $\dot{\gamma}=\sqrt{2D_{ij}D_{ij}}$ is the shear rate, and K_c, K_η are model constants (K_c=0.41, K_η=0.62).

For mold filling applications, the position of the flow front is determined using a pseudo-concentration method [14]. A smooth function $F(\mathbf{x},t)$ such that the critical value, F_c, represents the position of the interface. A value larger than F_c indicates a filled region. The pseudo-concentration function is transported using the velocity field provided by the solution of the momentum-continuity equations:

$$\frac{\partial F}{\partial t}+\mathbf{u}\cdot\nabla F=0 \qquad (9)$$

For velocity, no-slip boundary conditions are imposed on the cavity walls filled by the polymer, while on the unfilled part, a free boundary condition allows for the formation of the typical fountain flow. The heat transfer between the cavity and the mold is given by

$$q_m=h_c(T-T_m) \quad \text{on} \quad \Gamma_{\text{mold}}, \qquad (10)$$

where h_c is a surface heat transfer coefficient and T_m is the mold temperature.

FINITE ELEMENT SOLUTION

Model equations are discretized in time using a first order implicit Euler scheme. Linear continuous interpolation functions are used for all variables. At each time step, the global system of equations is solved in a partly segregated manner: momentum-continuity ($\mathbf{u}$,p), energy (T), solid phase concentration, and then the front tracking equation. The incompressible Navier-Stokes equations (1), (2) are solved using a Galerkin Least-Squares method [15], the energy equation is solved by a combined SUPG/GGLS (Streamline Upwind Petrov-Galerkin / Galerkin Gradient Least-Squares) method [15], and the front tracking equation is discretized by a SUPG method. A SUPG/GGLS method is also used for the solution of the solid phase concentration. The finite element formulation for the solid fraction equation is as follows:

$$\begin{aligned}
&\int_{\Omega}\left(\frac{\partial\phi}{\partial t}+\mathbf{u}\cdot\nabla\phi\right)w d\Omega-\int_{\Omega}\left(\mathbf{N}_c+\mathbf{N}_\eta\right)\cdot\nabla w d\Omega+\\
&\sum_K\int_{\Omega_K}\left(\frac{\partial\phi}{\partial t}+\mathbf{u}\cdot\nabla\phi\right)\tau\mathbf{u}\cdot\nabla w d\Omega_K+\\
&\sum_K\int_{\Omega_K}\nabla\left(\frac{\partial\phi}{\partial t}+\mathbf{u}\cdot\nabla\phi\right)\tau_\nabla\nabla w d\Omega_K=-\int_{\partial\Omega}\left(\mathbf{N}_c+\mathbf{N}_\eta\right)\cdot\hat{\mathbf{n}}w d\Gamma.
\end{aligned}\tag{11}$$

The integrals in the first row together with the right hand side term represent the standard Galerkin formulation with the diffusive flux integrated by parts. Integrals over the element interiors represent the stabilization terms. The term in the second row are from the SUPG formulation and stabilizes for the convection. The integrals in the third row are the GGLS stabilization and help avoid unphysical oscillations.

VALIDATION

In this section the solution algorithm is validated on cases for which both experimental and numerical data are available: circular Couette flow, piston driven flow and sudden contraction-expansion flow [6,10].

Circular Couette Flow

This application was the object of an experimental study by Abbott et al. [16] and reinvestigated both numerically and experimentally by Tetlow et al. [7]. The experimental apparatus has the inner rod (R_i) of 0.64 cm and the inner radius of the outer tube (R_o) of 2.38 cm. The particle radius a is 675 μm.

The initial particle concentration ϕ_0 is taken constant. As can be seen from equations (5)-(8) the steady state solution does not depend on the particle size but only on the initial value of the particle concentration. The numerical results given by the diffusive flux model are compared with experimental data in Figure 1 for initial particle concentrations of 0.45, 0.5 and 0.55. The 3D numerical results are in good agreement with the experimental data of Abbott et al. [16] and with the numerical results reported by Fang et al. [10].

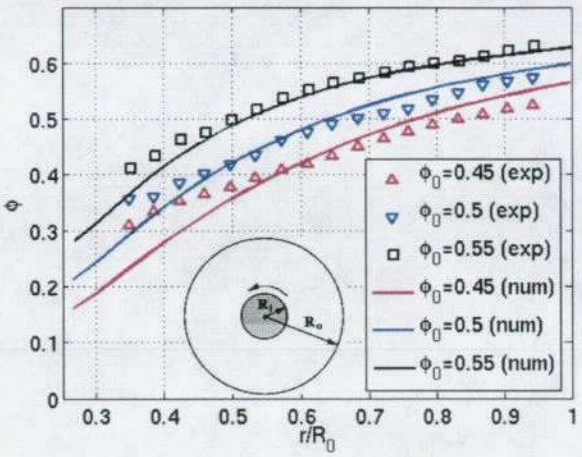

FIGURE 1. Comparison of model prediction with experimental particle concentration profiles of Abbott et al. [16].

Piston driven flow

This test case consists of displacing a fixed volume of suspension down a pipe by means of a piston. The material exhibits a similar behavior in injection molding where the suspension pushed by a piston forms a free surface. The uniformity of the suspension downstream of the piston will then affect the distribution of particles inside the molded part. An experimental study of this problem was performed by Subia et al. [6]. The piston radius is 2.54 cm and the pipe was filled with material on a length of 30 cm. The suspension contained 50% of spherical particles having 3178 μm in diameter. The piston moves from left to right at a speed of 0.0625 cm/s, while the pipe was held stationary. To avoid computation on a moving mesh a first computation was carried out on a fixed mesh by considering that the pipe moved from right to the left and the pistons were maintained fixed. The flow pattern after the piston was displaced with 15 piston diameters is shown in Figure 2. Segregation of solid particles for different positions of the piston is shown in Figure 3. As can be seen the solid fraction decreases in front of the piston that pushes the

suspension and is higher in the second half of the domain along the pipe axis. This is in agreement with experimental observation [6].

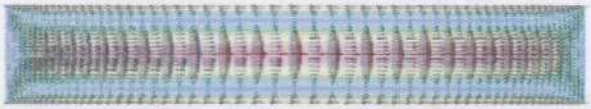

FIGURE 2. Velocity distribution for piston driven flow after 15 piston diameters (15D) for Eulerian approach.

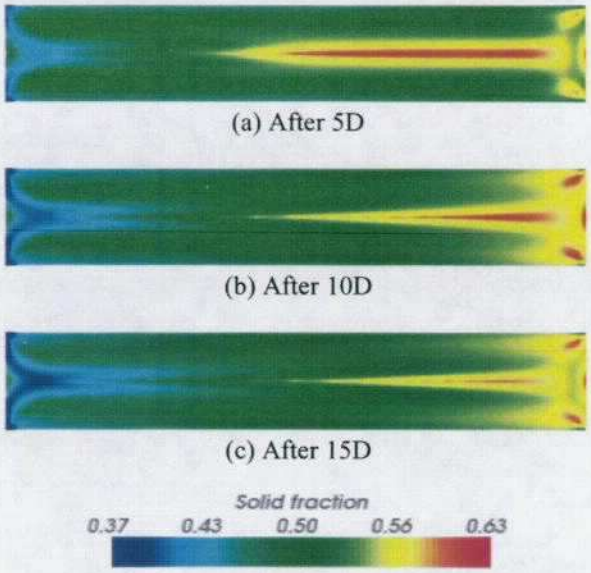

FIGURE 3. Distribution of solid fraction for various piston displacements (Eulerian approach).

The mean solid fraction on sections normal to the pipe axis was computed and plotted along the pipe axis in Figure 4. The results are compared with experimental data collected after the piston was displaced with 5 piston diameters. The numerical solution recovers correctly the segregation behavior, but slightly underestimates the change in the solid fraction. Simulation indicates that the segregation in front of a moving piston is produced quite rapidly and that a somehow steady distribution is attained after a 10D piston displacement.

As mentioned before, this problem describes well the behavior of the material during injection molding. However, simulation of the piston movement in material processing would not be possible in an Eulerian frame of reference, since the model includes both the moving piston and stationary parts as the mold cavity. Therefore a more general Arbitrary Lagrangian Eulerian (ALE) formulation needs to be considered. Here we have considered that the moving piston determines a deformation of the computational domain and hence of the mesh. The mesh is simply deformed (no remeshing) and the speed of the grid nodes is included into the advective velocity for the Navier-Stokes and scalar transport equations. Results using the ALE formulation for the piston driven flow with a free surface are shown in Figure 5. As can be seen the results are very close to those given by the Eulerian approach (Figure 4). Small differences are observed at the right end of the computational domain, where a non-planar free surface is present in the ALE solution and a flat no-slip surface is present in the Eulerian case. This test case indicates that the ALE approach performs well and can be used for injection molding applications.

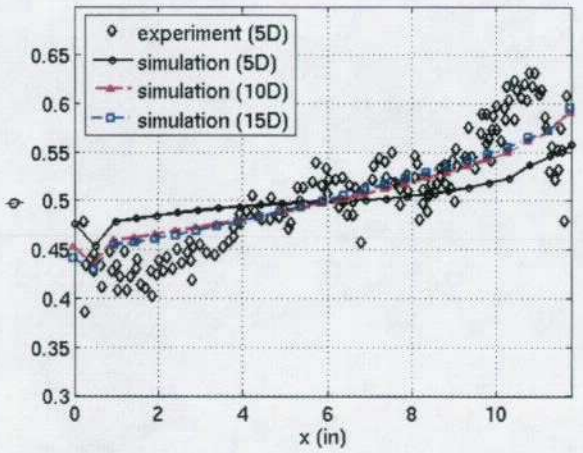

FIGURE 4. Mean solid fraction along the tube axis using an Eulerian approach.

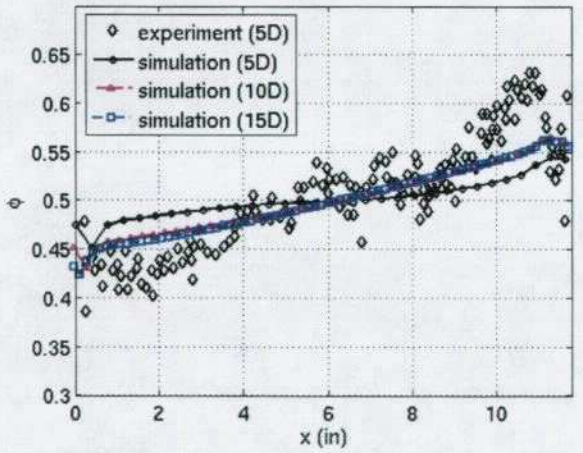

FIGURE 5. Mean solid fraction along the tube axis using an ALE approach.

Sudden contraction-expansion flow

This test case was the subject of an experimental study by Altobelli et al. [17]. The suspension is pushed by a piston from a reservoir pipe into a smaller diameter pipe and then into another larger catch pipe. The reservoir pipe and the catch pipe have a diameter of 5.08 cm, while the smaller pipe has an inner diameter of 1.27 cm. The smaller diameter pipe is 38 cm long. Initially 30 cm of the reservoir pipe, the entire smaller diameter pipe and 4 cm of the catch pipe were filled. The plunger was displaced at a constant velocity of 0.0625 cm/s, resulting in a mean velocity of 1 cm/s in the smaller pipe. The solid particles in the suspension were 50% by volume with a mean particle diameter of 675 μm.

The numerical solution was obtained using the ALE formulation. Figure 6 shows the mean solid fraction along the pipe axis after the piston has moved 2, 4 and 6 larger section diameters. Several observations can be drawn from these results. First we remark that the solid fraction decreases at the surface of the moving piston, observation made also in the case of the piston driven flow. Second we observe a sharp increase in the solid fraction just prior to the 4:1 contraction (x=-19cm). The solid fraction decreases then rapidly and reaches smaller values along the smaller diameter pipe. Third, we remark that at the 1:4 expansion, x=19cm, the solid fraction decreases before the section change and increases on a very small region after the expansion. In the catch pipe, x>19cm, the solid fraction is initially smaller than the mean value of 0.5, but increases towards the end of the pipe.

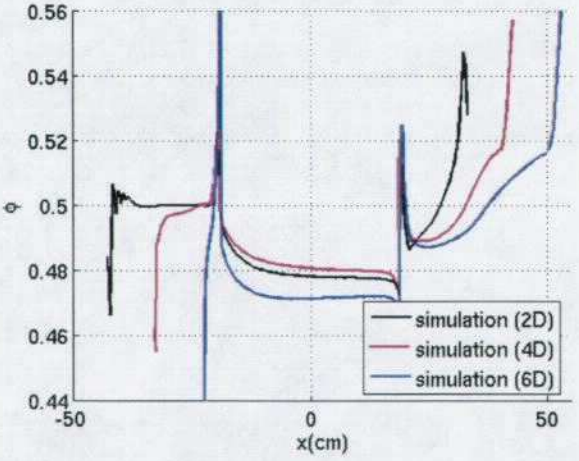

FIGURE 6. Sudden contraction-expansion flow: Mean solid fraction along the pipe axis using an ALE approach.

Figure 7 shows the solid fraction distribution in radial direction at various locations along the smaller diameter pipe. Results are plotted for x/L=0.1, 0.5 and 0.95, where L denotes the length of the smaller diameter pipe and x is the coordinate along the pipe measured in the sense of the flow (from the contraction towards the expansion). The results indicate that the solid fraction is larger near the axis of the pipe and decreases close to the pipe wall. We remark also that the segregation is more pronounced at x/L=0.5 and 0.95 than at the entry of the smaller diameter pipe. These observations agree well with the experimental findings of Altobelli et al. [17].

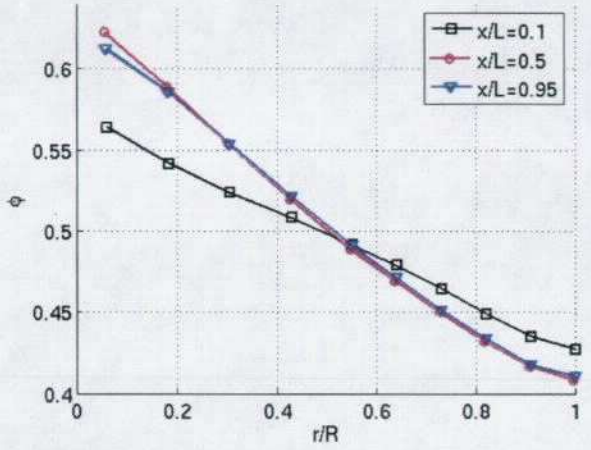

FIGURE 7. Solid fraction in radial direction at various locations along the smaller diameter pipe.

MOLD FILLING APPLICATION

In this application the ALE formulation is used to solve the injection molding of a rectangular plate. The plate is 8 cm by 6 cm and has 4 mm in thickness. The filling piston has a radius of 1 cm and his displacement is 13.2 cm. Filling of the plate is made through a circular gate with a radius of 2 mm. The suspension contains particles of 100 μm in radius and the initial solid fraction is uniform at 50%. Complete filling of the plate takes 10 s. The filling pattern and the solid fraction distribution is shown in Figure 8 after 1.7 s, 4 s, 7 s and respectively 10 s. The figure shows a cut along the symmetry plane parallel to the longest side of the plate in order to see the solid fraction distribution inside the part. The images on the left show the complete domain and the displacement of the piston during the filling is clearly seen. Images on the right are details of the flow inside the plate. Segregation of solid particles is apparent inside the pipe as previously observed for the piston driven flow case. This causes the material to enter the gate with a non-uniform solid fraction. Additional segregation is observed inside the gate where shear rates are highest. Finally, the molded part has higher solid fraction in the mid-plane and on the outside boundaries of the plate

and lower solid fraction on the upper and lower surfaces.

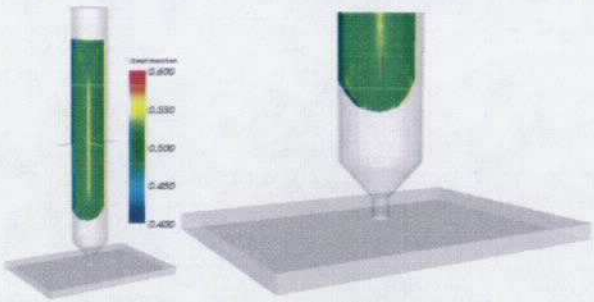

(a) t=1.7 s

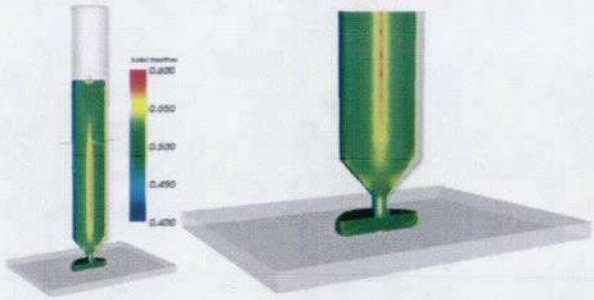

(b) t = 4 s

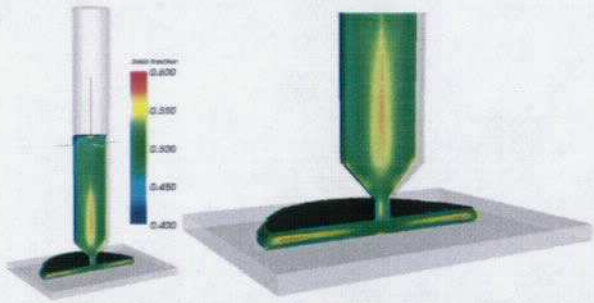

(c) t = 7 s

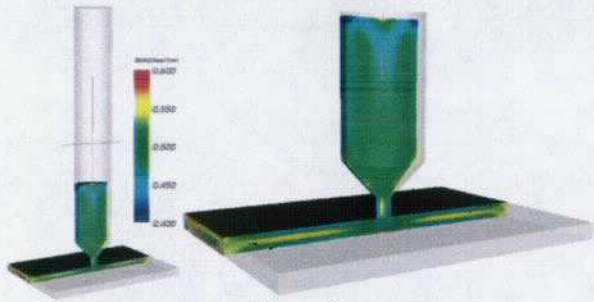

(d) t = 10 s

FIGURE 8. Distribution of solid fraction for the injection of a plate.

CONCLUSION

In this paper a three-dimensional finite element algorithm is shown for the solution of the flow of dense suspensions. The segregation of solid particles is described by a diffusive flux model. Validations cases show a good agreement with experimental data and previously published numerical solutions. The application to injection molding problems is done by using an ALE formulation. For the piston driven flow the ALE formulation is shown to provide similar results as an Eulerian approach on a fixed mesh, thus indicating that the procedure performs well. Application to the mold filling of a rectangular plate shows the ability to use this method to the solution of powder injection molding.

REFERENCES

1. T. Barrière, J.C. Gelin and B. Liu, *J. of Material Process. Techn., A*, **125-126**:518-524 (2002).
2. J. Petera and M. Kotynia, *Int. J. Heat Mass Transfer*, **47**:1483-1498, (2004).
3. M. Manninen and V. Taivassalo, On the mixture model for multiphase flow, *VTT Publications 288*, Finland (1996).
4. F. Pineau, F. Ilinca and J.-F. Hétu, A mixture approach for semisolid metal mold filling simulations, *Proc. MCWASP 2006*, TMS (2006).
5. R.J. Phillips, R.C. Armstrong, R.A. Brown, A.L. Graham and J.R. Abott, *Physics of Fluids, A*, **4**:30-40 (1992).
6. S.R. Subia, M.S. Ingber, L.A. Mondy, S.A. Altobelli and A.L. Graham, *Journal of Fluid Mechanics*, **373**:193-219 (1998).
7. N. Tetlow, A.L. Graham, M.S. Ingber, S.R. Subia, L.A. Mondy and S.A. Altobelli, *J. Rheol.*, **42**(2):307-327 (1998).
8. P. R. Nott and J.F. Brady, *J. Fluid Mech.*, **275**:157-199 (1994).
9. J.F. Morris and F. Boulay F., *J. Rheol.*, **43**(5):1213-1237 (1999).
10. Z. Fang, A.A. Mammoli, J.F. Brady, M.S. Ingber, L.A. Mondy and A.L. Graham, *Int. J. of Multiphase Flow*, **28**:137-166 (2002).
11. M.K. Lyon and L.G. Leal, *J. Fluid Mech.*, **363**:25-56 (1998).
12. N.C. Shapley, R.A. Brown and R.C. Armstrong, *J. Rheol.*, **48**(2):255-279 (2004).
13. F. Ilinca and J.-F. Hétu, *Int. Polym. Proc.*, **16**, 291 (2001).
14. F. Ilinca and J.-F. Hétu, *Int. J. Num. Methods Fluids*, **34**, 729-750 (2000).
15. F. Ilinca and J.-F. Hétu, *Int. J. Num. Methods Fluids*, **50**, 1445-1460 (2006).
16. J.R. Abbott, N. Tetlow, A.L. Graham, S.A. Altobelli, E. Fukushima, L.A. Mondy and T.S. Stephens, *J. Rheol.*, **35**(5):773-795 (1991).
17. S.A. Altobelli, E. Fukushima and L.A. Mondy, *J. Rheol.*, **41**(5):1105-1115 (1997).